Solar Phys
DOI 10.1007/s11207-015-0678-z

Galactic Cosmic Ray Density Variations in Magnetic Clouds

A. Belov[1] · A. Abunin[1] · M. Abunina[1] · E. Eroshenko[1] · V. Oleneva[1] · V. Yanke[1] · A. Papaioannou[2,3] · H. Mavromichalaki[2]

Received: 19 November 2014 / Accepted: 25 March 2015

Abstract We investigate the characteristics of Galactic cosmic rays in events associated with magnetic clouds that reach Earth. A mathematical model, capable of describing the distribution of the cosmic-ray density in a magnetic cloud is considered. We show that in most cases the behavior of the cosmic-ray density within magnetic clouds at 1 AU can be described accurately by a parabolic function of the distance to the center of the magnetic cloud measured in gyroradii. As expected, the majority of magnetic clouds modulate cosmic rays, resulting in a reduction of their density. However, there is a group of events (about one fifth of the total sample) in which the density of cosmic rays in a magnetic cloud increases. Furthermore, the extremum (a minimum or a maximum) of the cosmic-ray density is found closer to the cloud center and not at its edges. We consider a number of the factors contributing to the model and estimate the effect of each factor.

Keywords Galactic cosmic rays · Coronal mass ejections · Interplanetary coronal mass ejections · Magnetic clouds · Neutron monitors

✉ A. Papaioannou
atpapaio@phys.uoa.gr; atpapaio@astro.noa.gr

A. Belov
abelov@izmiran.ru

E. Eroshenko
erosh@izmiran.ru

H. Mavromichalaki
emavromi@phys.uoa.gr

1 IZMIRAN, Russian Academy of Sciences, Moscow, Russia

2 Nuclear and Particle Physics Department, Faculty of Physics, National and Kapodistrian University of Athens, Athens, Greece

3 IAASARS, National Observatory of Athens, 15236 Penteli, Greece

Published online: 10 April 2015

1. Introduction

Magnetic clouds (MCs) (Burlaga *et al.*, 1981; Burlaga, Plunkett, and Cyr, 2002) reach Earth in general with their initial structure intact, although they suffer some expansion. As was shown previously (*e.g.*, in Zhang, Hess, and Poomvises, 2013; Xie, Gopalswamy, and Cyr, 2013), all interplanetary coronal mass ejections (ICMEs), which are the interplanetary counterparts of coronal mass ejections (CMEs), arrive at Earth with a so-called flux-rope structure. However, this structure may not be reliably recorded in all events as a result of the relative position of the ICME and the observing point. If the observer (*e.g.* a satellite or Earth) passes through the front part of a disturbance (ICME), the flux-rope structure presents clear magnetic cloud characteristics (Wimmer-Schweingruber *et al.*, 2006). If the observer crosses the ICME at its flanks (and such events are the majority at 1 AU), as a rule, no magnetic clouds are observed, although a flux-rope structure can still be discernible. This means that there is a geometrical selection effect that strongly depends on the way the observer (*e.g.* a satellite or the Earth) crosses the ICME (Yashiro *et al.*, 2013). The second cause for the lack of a flux-rope structure can be the interaction of several CMEs. This can destroy the structure (*i.e.* lead to merged clouds). It was recently noted that an interaction of CMEs and their corresponding ICMEs results in a complex ejecta that in principle is very similar to an MC associated with an isolated CME, except for the long "tail" in the magnetic field and the hotter temperature throughout the ejecta (Lugaz and Farrugia, 2014). The flux-rope structure can also be destroyed by the interaction of the ICME with the leading solar wind (SW) (Zhang, Hess, and Poomvises, 2013), which most probably squeezes the flux-rope front. This in turn leads to the so-called "pancake effect", but it does not change the topology of the magnetic field lines. Thus, from satellite observations near Earth, we can practically see the filament structure that was created on the Sun – it is characterized by a strong magnetic field and a structure that is different from the one in disturbances that originate in the laminar solar wind. Furthermore, some MCs can have a large magnetic field component pointing to the south of the ecliptic (B_z negative), and therefore, they can initiate strong geomagnetic storms that result in an increase of the geomagnetic indices (Dst, Kp). Richardson and Cane (2010) compiled the most complete catalog of CMEs–ICMEs at present, including an identification of MCs, and demonstrated that CMEs with MCs are more geoeffective than other transient events: 43 % of the geomagnetic storms were caused by the arrival of an MC and only 18 % by ICMEs without an MC.

The main characteristics of a CME followed by an MC are shown in Figure 1, the start and end times of the MC are shown by two vertical lines. We gathered data from different sources and obtained a series of criteria for identifying the MCs (*e.g.*, Kim *et al.*, 2013):

- An increased intensity of the interplanetary magnetic field (IMF);
- Fewer IMF variations;
- An abnormally low proton temperature (T);
- A decrease of the solar wind velocity;
- A decrease of the plasma density;
- An increase of the Fe/O ratio;
- Bi-directional electron fluxes.

These features may not appear simultaneously, but the presence of two or three of them can already be used for the identification of an MC in the solar wind (*e.g.*, Gosling, 1990; Wimmer-Schweingruber *et al.*, 2006).

Magnetic clouds are closely related to cosmic-ray (CR) decreases, which are known as Forbush decreases (FDs) (Barnden, 1973; Belov *et al.*, 1976). FDs are caused by the

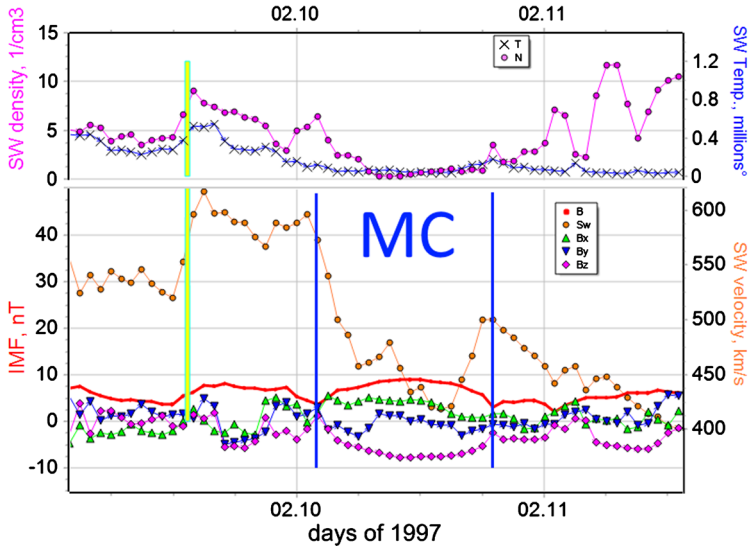

Figure 1 An example of magnetic cloud interplanetary data recorded in February 1997. The top panel represents the SW density (in cm^{-3}) and the SW temperature (in 10^6 K). The bottom panel displays the IMF intensity B (in nT) and its three components B_x, B_y, and B_z, as well as the SW speed (in $km\,s^{-1}$). The vertical solid blue lines denote the start and end of the MC, while the green and yellow vertical bars mark the sudden strong commencement (SSC).

expansion of partially closed magnetic structures in the solar wind (Lockwood, 1971; Cane, 1993; Belov, Eroshenko, and Yanke, 1997; Belov, 2009; Richardson and Cane, 2010), and since MCs are the most obvious examples of such a structure, it is natural to expect the strongest decrease in CR density exactly within MCs. The concept of the two-step FD is based on this idea (Barnden, 1973; Wibberenz *et al.*, 1988; Cane, 2000; Blanco *et al.*, 2013); the second, more dramatic decrease in CR density is connected with the MC. The influence of MCs on Galactic cosmic rays (GCRs) was considered in a number of works (Badruddin and Yadav, 1986; Zhang and Burlaga, 1988; Lockwood, Webber, and Debrunner, 1991; Cane, 1993, 2000; Singh and Badruddin, 2007; Quenby *et al.*, 2008; Abunin *et al.*, 2013; Blanco *et al.*, 2013) with ambiguous results. Most recently, Belov *et al.* (2014) presented a comprehensive work with statistical results on the connection of CMEs with FD characteristics.

The present work is different from previous research because we used data on the CR density of a certain rigidity (10 GV) outside the Earth's atmosphere and magnetosphere that were obtained with the Global Survey Method (GSM) (Belov *et al.*, 2005). In addition, the much larger number of events we considered allows a thorough statistical analysis and, finally, there are some methodological differences that we discuss below.

From the study of MCs we can understand the development of the solar wind disturbances and their possible geoeffectivity, since it is possible to predict the behavior of the B_z component, which is crucially important for the initiation of a geomagnetic storm. Bothmer and Schwenn (1998) attempted to employ such an approach by studying MCs with cylindrical models. This model was subsequently modified by Mulligan, Reinard, and Lynch (2013). Evidently, acquiring a valid and reliable model of MCs would enable predicting its further development from the beginning of the MC evolution; hence the implementation of such models is very important. In this work, we model MCs and analyze the arguments on which

the model is based. Moreover, Forbush effects (FEs) often develop in MCs, but until now no statistical study of the influence of MCs on GCRs has been conducted. Nonetheless, the first steps in this direction were recently taken in Abunin *et al.* (2013).

Apparently, a considerable part of MCs observed at 1 AU have a quasi-cylindrical geometry, and the strength of the IMF can be represented by a stretched cylinder (Mulligan, Reinard, and Lynch, 2013). This agrees with modern representations of the inner part of a CME, which is the original solar filament considered as a long cylindrical bundle of twisted field lines (a flux rope), and with observations of SW disturbances at Earth. Only a small near-Earth part of the MC can be considered and correspondingly treated as a cylinder. This is not possible for the full extension of the MC. Thus the cylinder representation can be used to model the near-Earth part of MCs and to predict the further development of the disturbance. Cylindrical models have been successfully used to represent the behavior of CRs in an MC (Kuwabara *et al.*, 2009). Hence, it is reasonable to assume that it is possible to isolate the influence of the near-Earth part of the ICME on CRs from the overall modulation caused by the sum of the interplanetary perturbations. In this work we consider only the behavior of the isotropic part of the CR variation (*i.e.* the density of CRs). It is natural to expect that the mechanism of FDs will be most effective directly within the MC owing to its expansion and relative isolation. This has been demonstrated in a number of case studies (*e.g.* Richardson and Cane, 2010; Papaioannou *et al.*, 2010, 2013; Abunin *et al.*, 2012; Blanco *et al.*, 2013). In this case, it is expected that the minimum of the CR density be observed at the central axis of the MC, while towards the surface of the MC the CR density should be increasing. The simplest function to simulate such a distribution is the parabola, but more complex functions derived from theoretical studies can be used. These functions coincide with a parabola, in first approximation, as we show below.

Magnetic clouds that engulf Earth often lead to magnetic storms. These storms can affect the CR variations that are registered by ground-level detectors. These so-called magnetospheric variations (Dorman, 2010) are observed as a sudden but small excess in the counting rate of the detectors and are caused by changes of the geomagnetic cut-off rigidities at the location of the detectors (Belov *et al.*, 2005). Evidently, such an increment in the counting rate of a detector may lead to undesirable effects in MC modeling and thus need to be considered as well. In this work we investigate and discuss the distribution of CRs within an MC.

2. Data and Methods

The analysis we present is based on the catalog of ICMEs that covers the time from 1996 to 2010 and was presented by Richardson and Cane (2010), hereafter RC2010. This is the only full catalog of interplanetary disturbances for these years and includes key parameters of interplanetary disturbances, their solar sources, and accompanying geomagnetic effects. We selected those ICMEs from RC2010 that were included in the list of magnetic clouds of *Wind* (http://wind.nasa.gov/mfi/mag_cloud_pub1.html) and/or are listed in Gosling (1990) and Huttunen *et al.* (2005). This has led to a sample of 99 events. Furthermore, the database on Forbush effects created by the Pushkov Institute of terrestrial magnetism, ionosphere and radio wave propagation (IZMIRAN), is based on the density and anisotropy variations of CR particles with 10 GV rigidity, obtained by the GSM (Belov *et al.*, 2005) using data from the world-wide neutron monitor network (around 50 stations). These variations of density and anisotropy of CRs are valuable and can effectively be used to study heliospheric processes, compared to the data of any single CR detector, since the GSM allows deriving characteristics of CRs outside the atmosphere and Earth's magnetosphere.

3. Discussion of the Results

The selected sample of events include both short- and long-lasting disturbances, very fast (slow) ICMEs, with an SW speed at Earth > 1000 km s^{-1} (< 400 km s^{-1}), with great or low IMF strength. The IMF strength can be very significant (up to 57 nT) or very modest (up to 8 nT). Only 62 out of 99 events started with the arrival of an interplanetary (IP) shock that was marked as a clear sudden storm commencement (SSC). Significant differences also arise in the events caused by different ICMEs. For example, in addition to the strongest ever recorded magnetic storms, our sample includes ten events in which the Kp-index did not even rise to level 4 (Kp < 4). The resulting CR variations were also very different. The strongest FD in history (with amplitude $A_F = 28$ %) is included in our selection, but also several weak FDs with no more than 0.5 % amplitude (all characteristics of the CR variations are calculated for a rigidity of 10 GV). As a result, it is clear from the characteristics of the 99 events with MCs that the mean amplitude of the FDs is large ($A_F = 3.4 \pm 0.4$ %) and that these FDs are accompanied, again, on average, by moderate magnetic storms ($A_{p_{\max}} = 98 \pm 9$ nT, and $Dst_{\min} = -103 \pm 8$ nT).

To highlight the dependence of the CR modulation upon the presence (or absence) of MCs, we compared the statistical results for our selected sample of 99 events (which are characterized by the presence of MCs) to the results of a control sample, ICMEs without an MC (around 150 events). This control sample includes events during the same time span (*i.e.* 1996 – 2010) with similar IP characteristics (*i.e.* intense IMF and high SW speed). This comparison showed that ICMEs with MCs modulate CRs more efficiently, leading to stronger FDs (as characterized by their amplitude, A_F [in %]), show a higher CR density decrement ($D_{\min}$) and a larger size of the CR anisotropy. This is expressed by the maximum value of the equatorial component of the first harmonic, $A_{xy_{\max}}$ and by the range of the north–south component, $A_{z_{\text{range}}}$ ($A_{xy_{\max}}$, $A_{z_{\text{range}}}$ [in %]). A similar trend was also identified in the geomagnetic indices (*e.g.* $Dst_{\min}$ [in nT], $A_{p_{\max}}$), but to a lesser extent. The comparison of all these parameters is presented in Table 1, where Column 1 refers to the selected parameter, Column 2 to the average values obtained for the sample of events with an associated MC and Column 3 to the average values obtained for the sample of events without an associated MC.

Here A_F is the magnitude of Forbush decrease (in %), $A_{xy_{\max}}$ the maximum equatorial component of the CR anisotropy vector (in %), $A_{z_{\text{range}}}$ the range of the changes of north–south component of the CR anisotropy vector (in %), $D_{\min}$ the maximum hourly decrement of the CR density, $V_m B_m$ the normalized product of the maximum SW velocity and the

Table 1 Mean CR parameters, measured in interplanetary space, and geomagnetic activity for disturbances with and without MC.

Parameter	Average for the sample of events with an MC	Average for the sample of events without an MC
A_F	3.36 ± 0.37	1.91 ± 0.16
$A_{xy_{\max}}$	2.03 ± 0.13	1.38 ± 0.08
$A_{z_{\text{range}}}$	2.04 ± 0.10	1.36 ± 0.06
$D_{\min}$	-0.93 ± 0.11	-0.44 ± 0.03
$A_{p_{\max}}$	97.87 ± 8.65	56.64 ± 3.51
$Dst_{\min}$	-102.6 ± 8.2	-56.5 ± 3.8
B_m	20.21 ± 1.07	18.01 ± 0.33
V_m	551.5 ± 16.5	652.2 ± 9.1
$V_m B_m$	6.05 ± 0.54	5.79 ± 0.07

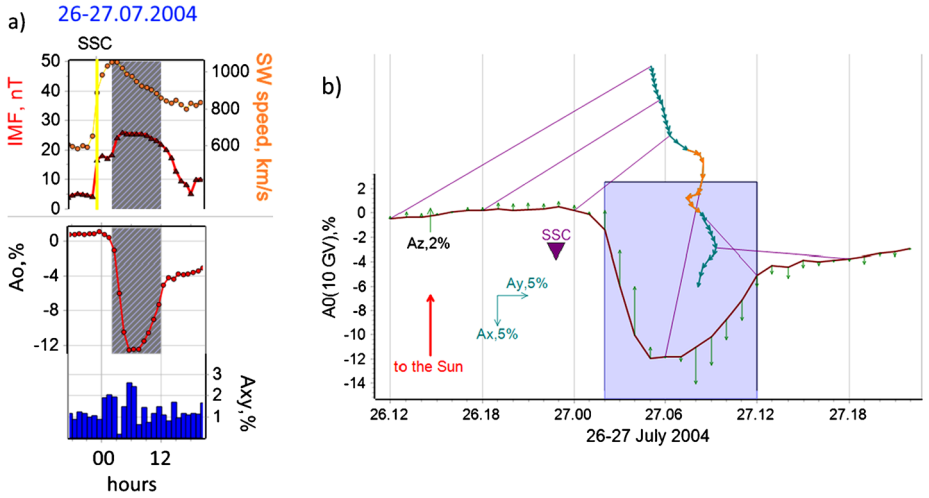

Figure 2 Example of a fast event with a clearly pronounced minimum in CR density inside the MC (26 – 27 July, 2004). IMF: intensity of the interplanetary magnetic field, A_0 – density of the CR with a rigidity of 10 GV, A_{xy} – equatorial component of the first harmonic of the CR anisotropy for particles of 10 GV, shown as a vector diagram in b) above the time profile of A_0, and A_z – north–south component of the anisotropy, shown as green vertical arrows on the time profile of A_0. The shaded/colored rectangles in all panels correspond to the MC duration. The orange arrows in b) represent the A_{xy} component during the MC.

IMF intensity, which is the most effective characteristic of the interplanetary disturbance to correlate with different parameters. This parameter is normalized as follows:

$$V_m B_m = \frac{V_{\max}}{V_0} \frac{B_{\max}}{B_0}, \tag{1}$$

where V_0 and B_0 are the typical parameters of the undisturbed interplanetary space. We take $V_0 = 400$ km s^{-1}, $B_0 = 5$ nT, $B_{\max}$ (in nT) and $V_{\max}$ (in km s^{-1}) as the maximum intensity of the IMF and the SW velocity in the disturbance.

Figures 2 – 5 illustrate examples of various ICMEs with an associated MC and their signatures. The figures correspond to the ICMEs of 26 – 27 July, 2004, 03 – 04 October, 2000, 07 – 08 August, 1996, and 20 – 22 February, 2000. The top panels of Figures 2a, 3a, 4, and 5 show the strength of the IMF [nT] (left scale, triangles) and the SW speed [km s^{-1}] (right scale, circles). The bottom panels present the variations of the CR density A_0 [in %] (left scale, filled circles) and A_{xy}, the equatorial component of the CR anisotropy [in %] (right scale, bars). Figures 2b and 3b present the isotropic part of the CR density variations at 10 GV rigidity, A_0 (solid line, in %), the equatorial component of the CR anisotropy A_{xy} (in %) as a vector diagram, the changes of the north–south component of the CR anisotropy A_z (in %) as vertical vectors that correspond to each hour of time. Thin lines connect the same times in the vector diagram (A_{xy}) and the solid line (CR density variations) every six hours. The shaded area in Figures 2 – 5 represents the time Earth spends inside the MC.

On 26 – 27 July, 2004 (Figure 2a, b), Earth was inside a fast ICME ($Vsw \approx 1000$ km s^{-1}) with a strong IMF (> 25 nT) with the maximum of the IMF observed in an MC. In this event the deep minimum of the CR density directly at the center of the MC is clearly visible. This event can be classified as two-step FD (Barnden, 1973; Cane, 2000). The first step is at the arrival of the SSC, labeled with the yellow vertical line, and the second step – which is

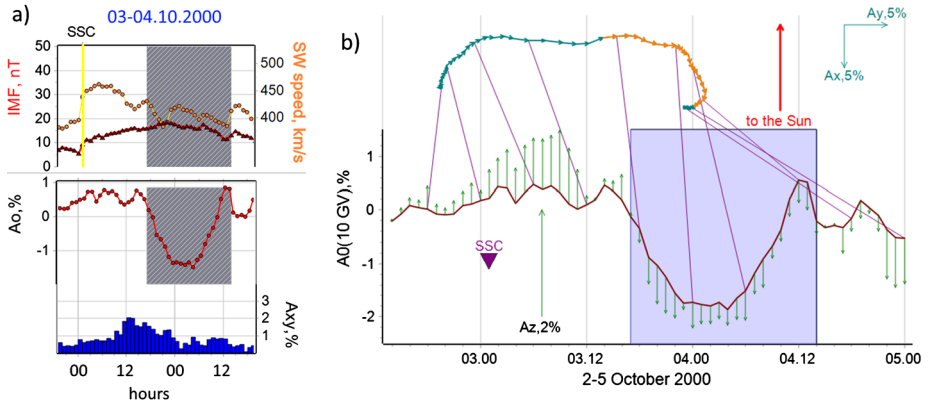

Figure 3 Example of the event with clearly visible minimum in CR density inside the MC upon a relatively low solar wind velocity (3 October, 2000). IMF: intensity of the interplanetary magnetic field, A_0 – density of the CR with a rigidity of 10 GV, A_{xy} – equatorial component of the first harmonic of the CR anisotropy for particles of 10 GV, shown as a vector diagram in b) above the time profile of A_0, and A_z – north–south component of the anisotropy, shown as green vertical arrows on the time profile of A_0. The shaded/colored rectangles in all panels correspond to the MC duration. The orange arrows in b) represent the A_{xy} component during the MC.

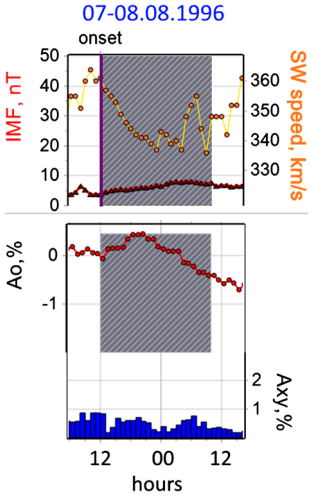

Figure 4 Example of event with increasing CR density inside the MC (7 August, 1996). IMF: intensity of the interplanetary magnetic field, A_0 – density of the CR with a rigidity of 10 GV, A_{xy} – equatorial component of the first harmonic of the CR anisotropy for particles of 10 GV, shown as a histogram in the lower panel of the figure. The shaded rectangle corresponds to the MC duration.

highly pronounced – begins with the entry into the MC, thus at the edge of the shaded area. A similar behavior of the CR density was observed on 03 – 04 October, 2000 (Figure 3a, b), although this event was connected with a rather slow ICME ($Vsw \approx 480-400$ km s^{-1}). There are many more examples with a similar CR density behavior. FEs both with a two-step structure and with the main density minimum within an MC are rather typical (Belov, 2009).

However, the presence of a magnetic cloud does not necessarily guarantee that an FD has a two-level structure (Jordan *et al.*, 2011). In our selected sample of events the main minimum of the CR density appears within an MC only in 67 out of the 99 cases (67.68 %). The minimum of the CR density is seen even less frequently at the center of the MC. Moreover,

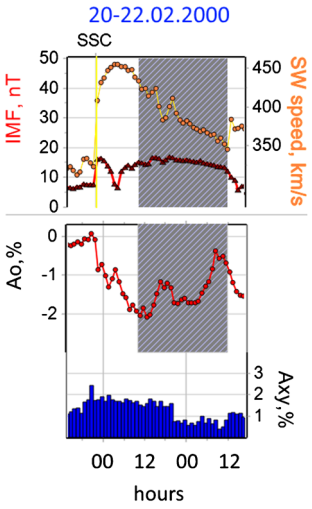

Figure 5 Example of event with a complicated MC structure (20 February, 2000). IMF: intensity of the interplanetary magnetic field, A_0 – density of CR with a rigidity of 10 GV, A_{xy} – equatorial component of the first harmonic of the CR anisotropy for particles of 10 GV, shown as a histogram in the lower panel of the figure. The shaded rectangle corresponds to the MC duration.

there were some events in which a local maximum was observed instead of a minimum of the CR density at the central part of the MC. One of these examples is presented in Figure 4. As in this example, in such abnormal events the intensity of the IMF in the MC is usually insignificant (< 15 nT). In some cases within an MC, the CR density is more complicated: it is characterized by the alternation of local maxima and minima (Figure 5, bottom panel). These examples show that the behavior of the CR density reflects not only an MC as a whole, but also detailed features of its structure.

Furthermore, MCs strongly influence the behavior of the first harmonic of CR anisotropy. As a rule, at the start of the MC and/or at its end, the amplitude as well as the direction of the anisotropy changes significantly. It is possible to observe these changes in the equatorial component of the anisotropy A_{xy} (in %) (Figures 2a and 3a, bottom panels, and Figures 2b and 3b, the vector diagram), and also in the north–south component A_z (in %) of the first harmonic of the CR anisotropy in the examples presented in this article (Figures 2b and 3b). Moreover, within an MC, systematic changes of the behavior of the CR anisotropy are usually observed. For the A_{xy} (in %) component it is characteristic to observe a rotation that typically is only in one direction (as in Figure 3b, orange arrows), although sometimes a change of direction is noted (*e.g.* Figure 2b). The north–south component A_z (in %) typically varies regularly within an MC, but a change of sign is observed very frequently at the center of the MC (see Figure 2b). A wide variety of MCs with high and low speed, with strong and weak IMF, and with variable duration result in FDs with different amplitudes and modulations. Examples of the CR density variations are presented in Figures 6 and 7, which are the result of the passage of MCs with different properties: fast (Figure 6, left column), slow (Figure 6, middle column), and complex (Figure 6, right column). These latter events present a complex behavior of the CR density at the center of the MC. In a number of events, an increase (Figure 7) is observed instead of a density minimum in the central part of the MC. Most probably, in a number of these configurations the regular structure of the magnetic field in the MC allows charged CR particles to penetrate its central part from remote eastern parts of the heliosphere that are not affected by the FD.

A crucial conclusion is that if an MC exists inside an interplanetary disturbance (*e.g.* ICME), this disturbance will significantly affect CRs. A number of reasons, often complementary, support this fact: 1a) when an MC is present in an ICME, the MC encounters Earth

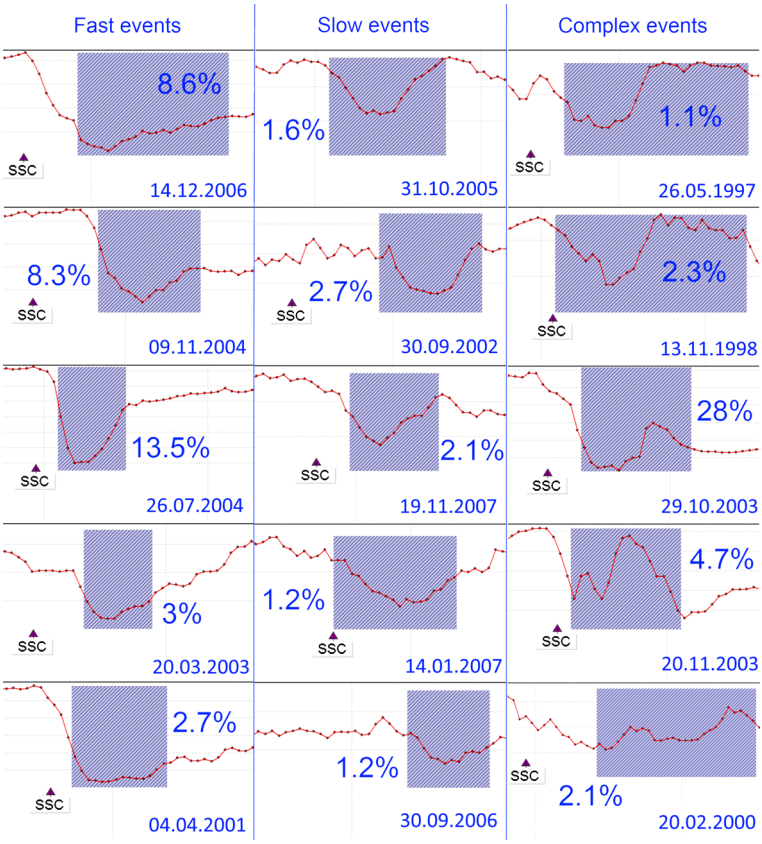

Figure 6 Examples of the Forbush-effect (FE) profiles caused by fast, slow, and complex ICMEs associated with MCs. The numbers in the panels correspond to the percentage of the maximum FE magnitude and the date of the event. Triangles mark the time of shock arrival at Earth (SSC). The shaded rectangles mark the time Earth spends within the MC. The CR density A_0 is presented as a function of time (red curve).

with a higher probability the stronger and closer to the center of the solar disk the source of the CME is; both of these factors increase the recorded magnitude of the FD (Abunina *et al.*, 2013). 1b) The mechanism that originates an FD occurs in an MC. For a disturbance that propagates in the IP medium without an MC, the following arguments can be put forward: 2a) the source of this disturbance is not a CME, but instead a coronal hole, which does not influence CRs as strongly. 2b) An MC was initially present, but as a result of the interaction with other structures (*e.g.* SW streams, other ICMEs), it lost its main properties and, in particular, its field became more irregular. The regular, well organized field influences CRs more effectively than a random field of the same intensity.

The behavior of the CR density within an MC reflects all these possibilities as a whole, but it can be also affected by its internal structure. This can be seen in the evolution of the CR density and the CR anisotropy vector in data of the worldwide network of neutron monitors using the GSM method (as shown in Figures 2 – 5). In most events, or at least in most events in our sample, the changes of the CR density within an MC is almost symmetric, with the CR density reaching a minimum at the center of the MC. This allows assuming a quasi-cylindrical structure. Other events in our sample present a regular behavior of the

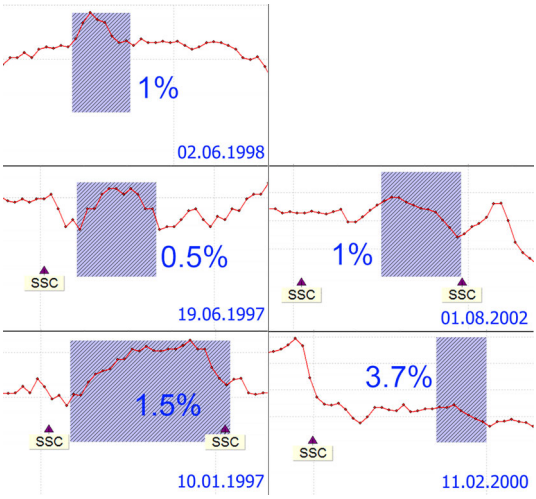

Figure 7 Examples of the effects (increasing density) on CR within an MC. In each panel the date of event and maximum change of CR density inside the MC are presented. Triangles mark the arrival of the shock at Earth. The shaded rectangles mark the time Earth spends within the MC. The CR density A_0 is presented as a function of time (red curve).

CR density, although it is more complex and has increases and decreases. These might be manifestations of the quasi-toroidal structure of some MCs.

4. Modeling the Cosmic-Ray Density Variations

4.1. Basic Principles of the Model

As mentioned above, the simplest function that can represent the distribution of the CR density in the quasi-cylindrical structure of an MC is a parabola. The real distribution may be different from a parabola, but other more essential conditions that cause a departure from this function can be present.

4.1.1. Expressing the Distance in Larmor Radii

Our study relies on hourly data of the CR density. As the ICME extends almost radially out from the Sun, we obtained an almost radial cut of the CR density distribution that we then studied extensively. This cut can be located anywhere in the cloud, but this does not limit the applicability of the parabolic representation of the CR density. When using hourly averaged data for modeling, we recall that when Earth crosses the interplanetary disturbance, it passes through different fractions depending on the speed of the disturbance during that hour. Moreover, it is important to consider specific issues of CRs. For charged particles (*e.g.* CRs), distances are not measured in kilometers (km) or astronomical units (AU), but in Larmor radii (gyroradii) ρ, which are defined by the rigidity of CR particles (R) and the intensity of the IMF (B). Therefore, an extended, long-lasting MC with a weak magnetic field can have a greater effect on cosmic rays than an MC that is narrower and short lived, but has a really strong field.

In an hour, the observer (*e.g.* Earth) travels in the interplanetary disturbance (in particular, in an MC) a distance in gyroradii: $X = cVB/R$, where V is the radial speed of the solar wind and c is a constant that depends on the units of V, B and R. A more symmetric distribution of the CR density in an MC is expected if the distance is given in gyroradii. This is clearly

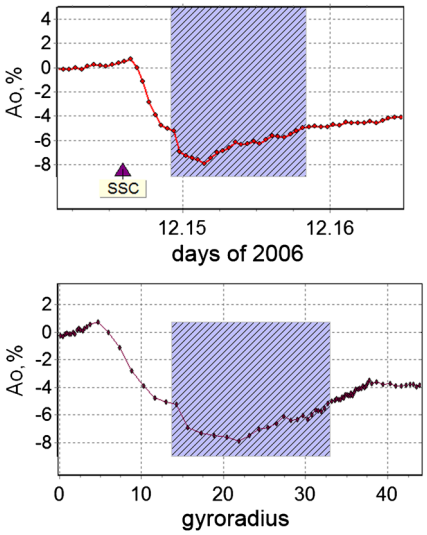

Figure 8 Example of the influence of an MC on CRs. Distribution of CR density (A_0) plotted as a function of time (top panel) and as a function of gyroradii (lower panel) of particles with a rigidity of 10 GeV. The shaded area shows the MC size for this event (15 December, 2006). The triangle marks the beginning of the geomagnetic storm.

visible in Figure 8, where the top panel presents an FD on 15 December, 2006; this was derived from the hourly NM data and from the corresponding modeled dependence for the same FD in gyroradii (bottom panel).

4.1.2. Influence of Magnetospheric Events

Geomagnetic storms can have an effect on CR variations that are registered by ground-level detectors. These are the so-called magnetospheric variations (Dorman, 2010). They are observed as a sudden but small excess in the counting rate of the detectors and are caused by changes of the geomagnetic cut-off rigidities, Rc, at the location of the detectors. It has been noted in many published cases that the variations of the cut-off rigidity and the corresponding variations of the CR counting rate are closely correlated with changes of the Dst index of geomagnetic activity. This correlation probably also extends to the variation of the CR density obtained by the GSM (*e.g.* see Belov *et al.*, 2005).

Taking into account both the change to gyroradii and the influence of magnetospheric events, the expected variation of the CR density in an MC can be written as

$$\delta = \frac{\Delta N}{N} = \alpha + \beta_1 X + \beta_2 X^2 + \beta_d Dst, \tag{2}$$

where α is a constant, β_1 is the trend coefficient, β_2 represents the main influence of the MC on CRs, β_d defines the contribution of the magnetosphere, and X is the distance measured in gyroradii.

This simple model was applied to the 99 events of our sample, and the parameters α, β_1, β_2, and β_d were defined for each hour. Figure 9 provides examples of the modeled distribution of the CR density in an MC. The upper panel corresponds to the event on 9 November, 2004. As can be clearly seen, the results of the model derived using Equation (2) (filled circles) agree very well with the observed CR density variations (dots). Nonetheless, the modeled distribution of the CR density does not always follow the observed CR density variations closely (Figure 9, lower panel). One of the main reasons for this discrepancy is that the simplified representation of an MC in the form of a quasi-cylinder in some cases

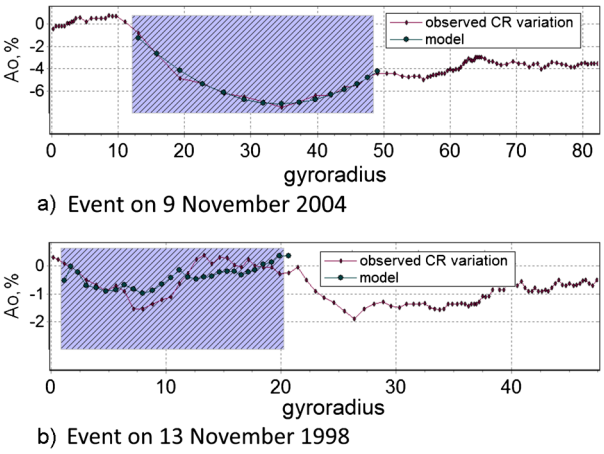

Figure 9 Comparison of the modeled and observed CR density variations for two different events: a) Event on 9 November, 2004, where a good agreement between model and data is clear. b) CR density variations are suggestive of a toroidal, rather than cylindrical, structure of the MC observed on 13 November, 1998, which causes a strong difference in the CR density variations from the model calculations.

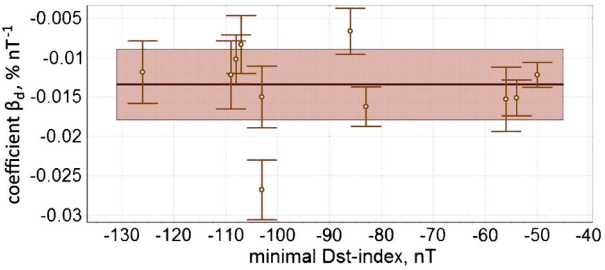

Figure 10 β_d in function of the minimum of the Dst index.

is not appropriate. In these cases, the dispersion (σ_2) in a least-squares fitting is large and the correlation coefficient, in contrast, is low. However, we recall that low-dispersion results are not always reliable. The number of hours that Earth spends within the MC varies in our sample from six to 64. It is thus clear that six hours (six points) are not enough to reliably determine the four model parameters. For most events the number of points is sufficient, however, since the average duration of an MC in our sample of events is 21 ± 1 hours.

4.2. Statistical Results

In this section, we present statistical results of the model and discuss the contribution of the coefficients in Equation (2). We did not consider MCs with length $< 4\rho$ and cases with large dispersion, $\sigma_2 > 0.3$ %. These criteria reduced our selection from 99 to 74 events. Thus, our simple model is applicable to most of the events.

Coefficient β_d defines the contribution of magnetospheric variations to the variations of the CR density. It is not always possible to obtain this coefficient precisely, since in many cases the magnetospheric variations of the CR density are too small to define β_d with sufficient accuracy. The events for which we were able to define β_d accurately are shown in Figure 10. β_d is depicted as a function of the minimum of the Dst index when Earth was within the MC. An averaged coefficient $\beta_{dm} = 0.0136 \pm 0.0016$ % $(\text{nT})^{-1}$ for these events is shown as a solid horizontal line. The shaded region is $\pm\sigma$ – where σ is a standard mean square deflection of distribution of the β_d coefficients. It is clear that the distribution of the points in Figure 10 and the error of the individual coefficients is within the limits of the standard deviation σ. There is no dependence of β_d on the magnitude of the Dst index.

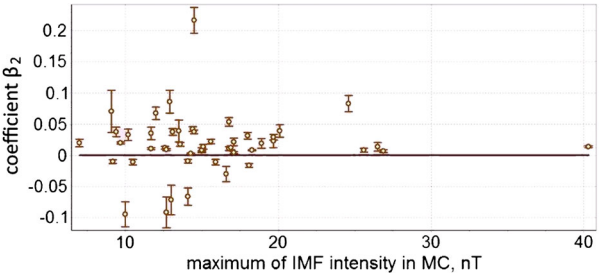

Figure 11 Dependence of β_2 on the interplanetary magnetic field intensity $B_{\max}$ inside the magnetic cloud.

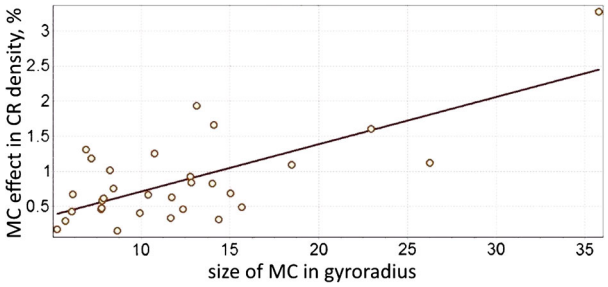

Figure 12 Dependence of the magnitude of the MC effect on cosmic-ray density (Forbush decreases) on the size of magnetic cloud (in gyroradii).

The point at -105 nT belongs to an event in February 1998. We had no formal reasons to exclude it from the analysis, but it is probable that in this event the structure of the MC was closer to toroidal than to cylindrical, and the parabolic dependence is an artifact due to a casual correlation of the CR density changes to the Dst index. Thus, this coefficient (about 0.27 % $(\mathrm{nT})^{-1}$) is apparently overestimated and should not be considered. The results allow us to assume that in all events (or, at least, in most of them) the relation between the magnetospheric variations and the CR density changes is approximately the same and is well defined by the average coefficient β_{dm}. Moreover, this coefficient can apparently be applied not only to the MCs, but also to variations in CR density of 10 GV rigidity particles obtained by the GSM during any period of time.

The coefficient β_2 is related to the proposed parabolic model. This coefficient reflects the main influence of the MC on the density of CRs. A positive coefficient corresponds to a decrease in CR density. If β_2 is small, comparable to the statistical error, it means that the MC only weakly influences CRs near Earth. But in other points of the heliosphere, this influence can be much more effective. For the analysis we selected 39 events for which $\beta_2/\sigma\beta_2 > 2$, so that the contribution of β_2 is statistically significant in the model. Figure 11 shows the dependence of β_2 on the maximum intensity of the IMF ($B_{\max}$) in the MC for the 39 selected events. Prevalence of positive β_2 (*i.e.* events with a local minimum in CR density within the MC) is obvious. Out of the 39 selected events, only nine events were found with $\beta_2 < 0$. These are the events with a local maximum in CR density within an MC. These negative values cannot be explained due to bad data or poor magnetospheric effects. The lack of dependence of β_2 on $B_{\max}$ is evident from Figure 11, but all negative β_2 were clearly observed in a relatively weak field, and for $B_{\max} > 18$ nT all β_2 are positive. Hence, in cases of strong magnetic field we always have "normal" FDs with a local minimum in CR density within an MC.

The influence of an MC on the CR density can be given by its size (in gyroradii). This is confirmed in Figure 12, where the magnitude of the influence of the MCs on CR density is shown for 31 events (correlation coefficient, cc = 0.70).

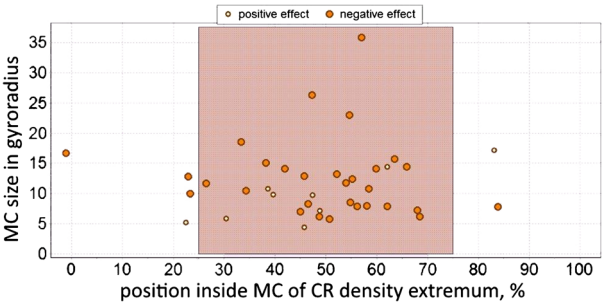

Figure 13 Location of the CR density extremes inside the magnetic clouds (in %).

The influence of most MCs on the density of CRs is insignificant. In 41 out of the 74 events this influence is < 0.3 % and in $50 < 0.5$ %. Weak effects like this cannot be shown by the data from a single detector. It is no surprise that some investigations concluded that MCs do not influence CRs. However, we believe that all CMEs/ICMEs influence CRs. Especially when they are observed at Earth. Effects of CMEs/ICMEs and MCs occur frequently, but are weak and difficult to detect.

The extremes (minimum or maximum) of the CR density occur closer to the center of the cloud more often than at its edges. This is evident in Figure 13. We divided all MCs into two subgroups: central (25 – 75 % of the cloud diameter) and lateral. Of the 39 events, 33 fall into the central group and only six in the lateral one. Figure 13 also shows that events with a positive effect (empty circles) have a maximum generally in the leading part of the MC. In the events with a negative effect (full circles), the minima of the CR density is distributed more evenly, but tend to be grouped in the trailing part of the MC.

5. Conclusions

We have shown that the presence of a magnetic cloud in an interplanetary disturbance as a rule increases the capability of the disturbance to affect Galactic cosmic rays. The CR density can be affected by an MC as a whole and also by its internal structure. The effects are visible in the behavior of the CR density and of the CR anisotropy vector obtained from data of the worldwide network of neutron monitors using the GSM method.

In a large number of events in our sample, the CR density changes within an MC, providing an almost symmetric picture, with the CR density minimum at the MC center. This allowed us to assume a quasi-cylindrical structure for the MC. Events in which the behavior of the CR density remained regular but became more complex with alternate increases or decreases are frequent. These events can be an indication of the quasi-toroidal structure of some MCs.

In most cases (but not in all), the distribution of the CR density within MCs at Earth can be described by a simple parabolic dependence on the distance to the MC center expressed in gyroradii. Most (but not all) MCs affect CRs and decrease their density, although there is a group of events (about one fifth) in which the CR density increases within an MC.

We determined a quantitative relation between the CR density variations during magnetospheric effects and the Dst index. We found that in all the events the relation of the Dst index with the changes of the CR density is approximately the same. This relation is given by the average coefficient β_2 we obtained, which can apparently be applied not only to MCs, but also to any variation of the CR density for a rigidity of 10 GV during any period.

Furthermore, there is no obvious dependence of the CR density variations on the maximum intensity of IMF (B_{max}), measured within a magnetic cloud. However, we showed that all positive effects (CR density increases in MCs) are observed in rather weaker field values, and for $B_{max} > 18$ nT all variations of the CR density are negative; *i.e.*, for a strong magnetic field we always have "normal" FDs with a local minimum in CR density within an MC.

Finally, the extremes (minimum or maximum) of the CR density appear more frequently closer to the center of the cloud than at its edges. Events with a positive effect have a maximum generally in the leading part of an MC. In the events with a negative effect, the minima of the CR density is distributed more evenly, but tend to be grouped in the trailing part of the MC.

Acknowledgements The authors would like to thank the anonymous referee, whose thoughtful comments contributed significantly to this article. Furthermore, the authors are thankful to collaborators of the worldwide network of CR stations for providing the data and continuously monitoring of the neutron component: http://cr0.izmiran.ru/ThankYou/. The NMDB database (www.nmdb.eu), founded under the European Union's FP7 programme, is gratefully acknowledged (contract no. 213007) for the provision of data.

References

Abunin, A.A., Abunina, M.A., Belov, A.V., Eroshenko, E.A., Oleneva, V.A., Yanke, V.G.: 2012, *Geomagn. Aeron.* **52**, 292.
Abunin, A.A., Abunina, M.A., Belov, A.V., Eroshenko, E.A., Oleneva, V.A., Yanke, V.G., Mavromichalaki, H., Papaioannou, A.: 2013 In: *Proc. 33rd Int. Cosmic Ray Conf.*, id-198.
Abunina, M.A., Abunin, A.A., Belov, A.B., Eroshenko, E.A., Asipenka, A.C., Oleneva, V.A., Yanke, V.G.: 2013, *Geomagn. Aeron.* **53**, 13.
Badruddin, Y.R.S., Yadav, N.R.: 1986, *Solar Phys.* **105**, 413.
Barnden, L.R.: 1973 In: *Proc. 13th Int. Cosmic Ray Conf.* **2**, 1277.
Belov, A.V.: 2009, In: Gopalswamy, N., Webb, D. (eds.) *Proc. IAU Symp.* **257**, Cambridge University Press, Cambridge, 439.
Belov, A., Eroshenko, E., Yanke, V.: 1997 In: *Proc. 25th Int. Cosmic Ray Conf.* **1**, 437.
Belov, A., Dorman, L., Eroshenko, E., Ivanov, K., Inozemtseva, O., Kulanina, G., Mikerina, N.: 1976, *Geomagn. Aeron.* **16**, 355.
Belov, A.V., Baisultanova, L., Eroshenko, E., Yanke, V., Mavromichalaki, H., Plainaki, C., Mariatos, G., Pchelkin, V.: 2005, *J. Geophys. Res.* **110**, A09S20. DOI.
Belov, A., Abunin, A., Abunina, M., Eroshenko, E., Oleneva, V., Yanke, V., Papaioannou, A., Mavromichalaki, H., Gopalswamy, N., Yashiro, S.: 2014, *Solar Phys.* **289**, 3949. DOI.
Blanco, J.J., Catalan, E., Hidalgo, M.A., Medina, J., García, O., Rodríguez-Pacheco, J.: 2013, *Solar Phys.* **284**, 167. DOI
Bothmer, V., Schwenn, R.: 1998, *Ann. Geophys.* **16**, 1.
Burlaga, L.F., Plunkett, S.P., St. Cyr, O.C.: 2002, *J. Geophys. Res.* **107**, 1266.
Burlaga, L., Sittler, E., Mariani, F., Schwenn, R.: 1981, *J. Geophys. Res.* **86**, 6673.
Cane, H.: 1993, *J. Geophys. Res.* **98**, 3509.
Cane, H.: 2000, *Space Sci. Rev.* **93**, 55.
Dorman, L.: 2010, *Cosmic Rays in the Magnetosphere of the Earth and Other Planets*, Springer, Dordrecht.
Gosling, J.T.: 1990, *Geophys. Monogr.* **58**, 343.
Huttunen, K., Schwenn, R., Bothmer, V., Koskinen, H.: 2005, *Ann. Geophys.* **23**, 625.
Jordan, A.P., Spence, H.E., Blake, J.B., Shaul, D.N.A.: 2011, *J. Geophys. Res.* **116**, A11103. DOI.
Kim, R.-S., Gopalswamy, N., Cho, K.-S., Moon, Y.-J., Yashiro, S.: 2013, *Solar Phys.* **284**, 77. DOI
Kuwabara, T., Bieber, J., Evenson, P., Munakata, K., Yasue, S., Kato, C., Fushishita, A., *et al.*: 2009, *J. Geophys. Res.* **114**, A05109. DOI.
Lockwood, H.: 1971, *Space Sci. Rev.* **12**, 658.
Lockwood, J.A., Webber, W.R., Debrunner, H.: 1991, *J. Geophys. Res.* **96**, 11587.
Lugaz, N., Farrugia, C.J.: 2014, *Geophys. Res. Lett.* **41**, 769.
Mulligan, T., Reinard, A.A., Lynch, B.J.: 2013, *J. Geophys. Res.* **118**, 1410.
Papaioannou, A., Malandraki, O.E., Belov, A., Skoug, R., Mavromichalaki, H., Eroshenko, E., Abunin, A., Lepri, S.: 2010, *Solar Phys.* **266**, 181. DOI

Papaioannou, A., Belov, A.V., Mavromichalaki, H., Eroshenko, E., Yanke, V., Asvestari, E., Abunin, A., Abunina, M.: 2013, *J. Phys. Conf. Ser.* **409**, 012202.
Quenby, J.J., Mulligan, T., Blake, J.B., Mazur, J.E., Shaul, D.: 2008, *J. Geophys. Res.* **113**, A10102.
Richardson, I.G., Cane, H.: 2010, *Solar Phys.* **264**, 189. DOI
Singh, Y.P., Badruddin: 2007, *J. Geophys. Res.* **112**, A02101. DOI.
Wibberenz, G., Le Roux, J., Potgieter, M., Bieber, J.: 1988, *Space Sci. Rev.* **83**, 309.
Wimmer-Schweingruber, R.F., Crooker, N.U., Balogh, A., Bothmer, V., Forsyth, R.J., Gazis, P., Gosling, J.T., *et al.*: 2006, *Space Sci. Rev.* **21**, 177.
Xie, H., Gopalswamy, N., St. Cyr, O.C.: 2013, *Solar Phys.* **284**, 47. DOI
Yashiro, S., Gopalswamy, N., Mäkela, P., Akiyama, S.: 2013, *Solar Phys.* **284**, 5. DOI
Zhang, G., Burlaga, L.F.: 1988, *J. Geophys. Res.* **93**, 2511.
Zhang, J., Hess, P., Poomvises, W.: 2013, *Solar Phys.* **284**, 89. DOI